SOCS3 in retinal neurons and glial cells suppresses VEGF signaling to prevent pathological neovascular growth

Title: Retinal SOCS3 in neurons and glial cells suppresses VEGF signaling to prevent pathologic neovascular growth

Authors: Ye Sun[1], Meihua Ju[1], Zhiqiang Lin[2], Thomas W. Fredrick[1], Lucy P. Evans[1], Katherine T. Tian[1], Nicholas J. Saba[1], Peyton C. Morss[1], William T. Pu[2], Jing Chen[1], Andreas Stahl[3], Jean-Sébastien Joyal[4], Lois E. H. Smith[1*]

One Sentence Summary: Neuronal/glial SOCS3 is a novel regulator of neurovascular interaction and suppresses pathologic retinal angiogenesis through titration of STAT3 mediated VEGF signaling.

Affiliations:

[1]Department of Ophthalmology, Harvard Medical School, Boston Children's Hospital, 300 Longwood Ave, Boston, MA 02115, USA;

[2]Department of Cardiology, Harvard Medical School, Boston Children's Hospital, 300 Longwood Ave, Boston, MA 02115, USA;

[3]University Eye Hospital Freiburg, Killianstr. 5, Freiburg 79106, Germany;

[4]Department of Pediatrics, Centre Hospitalier Universitaire (CHU) Sainte-Justine Research Center, Université de Montréal, Montréal, Québec H3T1C4, Canada;

[*]**To whom correspondence should be addressed**: Lois E. H. Smith, MD, PhD, Department of Ophthalmology, Boston Children's Hospital, Harvard Medical School, 300 Longwood Avenue, Boston, MA 02115, USA. Tel: 617 919 2529. Email: lois.smith@childrens.harvard.edu

Abstract

Accumulating evidence indicates that retinal neuroglia and neural cells contribute to neovascularization in proliferative retinopathy, but the controlling molecular interactions are not well known. We identified a mechanism by which neurons influence neovascularization through suppressor of cytokine signaling 3 (SOCS3) in neurons and glial cells. We found that *Socs3* expression was increased in the retinal ganglion cell layer and inner nuclear layer after oxygen-induced retinopathy. Neuronal/glial *Socs3* deficient mice with oxygen-induced retinopathy had significantly increased pathologic retinal neovascularization and reduced vaso-obliterated retinal areas, suggesting that loss of neuronal/glial SOCS3 increased both retinal vascular re-growth and pathological neovascularization. In response to oxygen-induced retinopathy, retinal vascular endothelial growth factor A *(Vegfa)* expression was higher in neuronal/glial *Socs3* deficient mice than in than *Socs3 flox/flox* controls indicating that neuronal and glial *Socs3* suppressed *Vegfa* during pathologic conditions. Lack of neuronal/glial SOCS3 resulted in greater phosphorylation and activation of STAT3, which led to increased expression of its gene target *Vegfa,* and increased endothelial cell proliferation. In summary, neuronal/glial SOCS3 suppresses endothelial cell activation through suppression of STAT3-mediated neuronal/glia VEGF secretion, resulting in less endothelial proliferation and angiogenesis. These results show that neuronal/glial SOCS3 regulates neurovascular interaction and pathologic retinal angiogenesis by titrating VEGF signaling.

Keywords SOCS3; Neovascularization; VEGF; Neurovascular interaction

Introduction

Neurovascular interactions are important in the maintenance of the nervous system, and defects in this relationship can lead to disease, such as stroke (1), Alzheimer's disease (2), and epilepsy (3). In the retina, part of the central nervous system, accumulating evidence suggests that dysregulated cross talk between the vasculature and retinal neuroglia, photoreceptors, and other neural cells in diabetes might contribute to the pathogenesis of diabetic retinopathy (4-6). Similarly, the immature retinas of preterm neonates are susceptible to insults that disrupt both neural and vascular growth, leading to proliferative retinopathy of prematurity (7). While many factors have been suggested to mediate neurovascular crosstalk, including growth factors, hydrogen, potassium, neurotransmitters, adenosine, arachidonic acid metabolites, nitric oxide, neurotrophins and glutamate (4), we specifically investigated neuronal/glial suppressor of cytokine signaling 3 (SOCS3), a negative feedback regulator of inflammation and growth factor signaling (8) as a potential regulator of pathological retinal vessel growth.

SOCS3 inhibits the cytoplasmic effectors Janus kinase/signal transducers and activators of transcription (JAK/STAT) kinase and deactivates tyrosine kinase receptor signaling (9). It increases endothelial cell apoptosis (10). Neuronal SOCS3 deletion promotes optic nerve regeneration in adult mice (11). We have previously shown that vascular SOCS3 deletion (Tie2-Cre driven) is an inhibitor of pathologic angiogenesis (12). However, the role of neuronal SOCS3 in controlling neurovascular coupling-mediated pathologic retinal angiogenesis *in vivo* is unknown.

Systemic deletion of *Socs3* is embryonically lethal (13). We generated a conditional knockout of *Socs3* in retinal neurons and glia using a *Cre/loxP* site-specific DNA recombination fate mapping strategy. *Socs3* is deleted in neuronal/glial cells by crossing mice expressing the Cre recombinase transgene under the control of the *nestin* promoter with mice carrying *Socs3/loxP* (*Socs3*$^{flox/flox}$;*Nestin*$^{Cre/+}$, *Socs3 cKO*). Pathologic retinal angiogenesis in these mice was studied using a mouse model of oxygen-induced retinopathy (OIR) (14). In the OIR model, mice are exposed to 75% oxygen to induce vessel loss (phase I) followed by exposure to room air from P12-17 when the now avascular retina becomes hypoxic stimulating pathological neovascularization (phase II). When OIR is induced, *Socs3 cKO* mice showed significantly greater pathologic retinal neovascularization than littermate *flox/flox* controls (*Socs3f/f*); however normal retinal vascular growth during development was unaffected. These results suggested that neuronal/glial SOCS3 suppressed retinal angiogenesis in stress pathologic conditions but was dispensable in physiologic vascular development. Lack of SOCS3 in retinal neuronal and glial cells increased neuronal STAT3 activation and promoted vascular endothelial growth factor (VEGF) production in neuronal cells to increase signaling in endothelial cells, leading to proliferative retinopathy. Therefore, neuronal/glial SOCS3 controls the release of growth factors, which mediate vascular growth specifically in pathologic contexts.

Results

Socs3 mRNA was localized in neuronal layers in the retinas.

To examine the role of neuronal SOCS3 in controlling pathologic retinal angiogenesis, we generated pathological neovascularization in a mouse model of OIR (**Figure 1A**). To localize

Socs3 expression in mouse retinas with OIR, the retinal layers were laser-capture microdissected (**Figure 1B**) and each isolated layer assessed for specific mRNA expression with qPCR. In P17 retinas with OIR, *Socs3* mRNA expression is highly increased in proliferative vessels (12). We showed that *Socs3* mRNA expression was also highly increased in the retinal ganglion cell (RGC) layer and inner nuclear layer (INL) without any change in the outer nuclear layer (ONL) compared with age-matched controls exposed to room air.

Neuronal/glial Socs3 attenuated pathologic neovascularization in OIR

The *nestin Cre* recombination appears in most neural and glial cells within the retina (15-17). To explore the role of neuronal/glial Socs3 in pathologic retinal angiogenesis, we generated conditional *Socs3* knockout mice driven by *nestin Cre* (*Socs3 cKO*). Decreased *Socs3* levels were confirmed with western blot in *Socs3 cKO* retinas (**Figure 1C**). To confirm the knockdown of *Socs3* in INL and RGC layers in *Socs3 cKO* retinas, we crossed *Socs3 cKO* mice with $ROSA^{mT/mG}$ reporter mice. $ROSA^{mT/mG}$ is a cell membrane-targeted, two-color fluorescent Cre reporter allele, expressing cell membrane-localized tomato red fluorescence in widespread cells/tissues prior to Cre recombinase exposure, and cell membrane-localized green fluorescence in Cre recombinase expressing cells (and future cell lineages derived from these cells). We found *nestin Cre* recombination labeled with green fluorescence appeared in most neural/glial cells especially in the INL and RGC layers indicating that *Socs3* was knocked out in the INL and RGC layers in *Socs3 cKO* retinas (**Figure 1D**).

Our previous publication (17) showed that in mice expression of Cre recombinase in nestin-expressing cells does not influence vaso-obliteration and neovascularization in retinas with OIR.

Socs3 cKO retinas with OIR showed ~40% more retinal neovascularization than littermate *Socs3 f/f* control retinas with OIR at P17 (**Figure 2A)**. There was also significantly less vaso-obliterated retinal area suggesting increased vascular regrowth into vaso-obliterated areas from P12 to P17 (**Figure 2A)**. *Socs3 cKO* and *Socs3 f/f* mice had comparable amounts of vaso-obliterated retinal area (**Figure 2B**) at P12 in OIR indicating that lack of *Socs3* did not influence vessel loss during hyperoxia. To investigate whether lack of *Socs3* in the INL and RGC layers influences normal developmental vascular growth, we compared the whole superficial vascular area on flat mounts at P7 (**Figure 2C**) and at P30 after full vascular development compared the three vascular layers (superficial, intermediate and deep) in cross sections and with confocal microscopy in whole retina (**Figure 2D**). There was no difference in the superficial vascular area at P7 during development nor any differences in any of the three vascular layers in adult mice between *Socs3 f/f* and *Socs3 cKO* groups. The thickness of each retinal layer in live adult mice measured using optical coherence tomography (OCT), was comparable in *Socs3 f/f* and *Socs3 cKO* retinas (**Figure 2E**). These data suggested that loss of neuronal/glial *Socs3* attenuated pathologic neovascularization in OIR but did not affect developmental vascular growth.

Neuronal/glial Socs3 deficiency increased retinal VEGF expression

In the OIR model, mice are exposed to 75% oxygen to induce vessel loss followed by room air from P12-17 when the avascular retina becomes relatively hypoxic and pathological neovascularization occurs. During the relatively hypoxic and proliferative phase from P12-P17, *Vegfa* mRNA levels increase mostly in Müller cells of the inner retina, which contributes to pathologic neovascularization (18-20). We confirmed that *Vegfa* expression was higher in neuronal and glial cells in the RGC and INL layers in retinas with OIR than in age-matched

normoxic controls (**Figure 3A**). Next we explored potential neuronal/glial SOCS3 regulation of VEGF expression. In the P17 mice with OIR, retinal *Vegfa* mRNA expression was significantly higher in *Socs3 cKO* than that in *Socs3 f/f* mice with OIR (**Figure 3B**), suggesting that neuronal/glial *Socs3* deficiency promotes neuronal/glial *Vegfa* expression in retinas with OIR. Murine VEGFA is expressed in at least three distinct isoforms of 120, 164 and 188 amino acids, which are generated by alternative transcription from a single gene locus (21). Real time PCR results (**Figure 3C**) showed that neuronal/glial *Socs3* deficiency promoted *Vegfa* isoform 120 and 164, but not 188 expression in retinas with OIR. Increased VEGF-A (isoform 164) protein abundance was confirmed by western blot (**Figure 3D**) and immunohistochemistry staining showed that neuronal/glial Socs3 deficiency promoted VEGF-A (isoform 164) protein induction mainly in the RGC and INL layers in retinas with OIR (**Figure 3E**).

Neuronal/glial Socs3 deficiency feedback enhanced STAT3 activation

Our data suggested that in OIR, neuronal/glial SOCS3 controlled in part the increased production of VEGF, a key angiogenic protein, that is secreted from neuronal and glial cells and that acts on vascular endothelial cells resulting in retinal neovascularization. Hypoxia-inducible factor 1-alpha (HIF-1α) is stabilized during hypoxia and transcriptionally activates *Vegf* expression (22). However, in retinas with OIR from *Socs3 cKO* mice and littermate *Socs3 f/f* controls the mRNA expression of other HIF-1α target genes involved in angiogenesis including erythropoietin (*Epo*), angiopoietin-like 4 (*Angptl4*), angiopoietin 1 (*Ang1*), platelet-derived growth factors alpha (*PDGFα*) and transforming growth factor beta (*TGFβ*) (**Figure 4A**), and HIF-1α protein expression (**Figure 4B**) was similar, indicating that HIF-1α might not primarily regulate the

increased VEGF expression in neuronal/glial *Socs3*-deficient retinas with OIR compared with *Socs3 f/f* control retinas.

SOCS3 binds to both the kinase JAK and the interleukin-6 receptor, which inhibits the activation of STAT3 (23). STAT3 activation regulates the expression of *Vegf* (24, 25). We examined the activation of STAT3 in response to neuronal/glial *Socs3* expression. Phosphorylated STAT3, the active form of STAT3, was 3.5 fold higher in P17 *Socs3 cKO* retinas with OIR than in *Socs3 f/f* controls (**Figure 4C**) and was increased mainly in the INL and RGC layers (**Figure 4D**). These results indicated that STAT3 activation was increased by neuronal/glial SOCS3 deficiency, which may have led to the observed increase in *Vegfa*. Therefore, neuronal/glial Socs3 is an important regulator of pathologic angiogenesis that may act through STAT3-mediated *Vegf* expression.

Neuronal/glial Socs3 deficiency increased endothelial proliferation and ErK phosphorylation.

VEGF stimulates endothelial cell proliferation to promote angiogenesis. We found that a proliferation marker Ki67 co-localized with the endothelial cell marker, isolectin IB4, and was significantly increased in *Socs3 cKO* retinas with OIR compared with *Socs3 f/f* controls with OIR indicating that neuronal/glial *Socs3* deficiency increased vascular endothelial cell proliferation (**Figure 5A and 5B**). We further explored whether VEGF can induce activation of ERK (26) in neuronal/glial *Socs3* deficient retinas with OIR. Phosphorylated ERK was higher in *Socs3 cKO* P17 retinas with OIR than in *Socs3 f/f* retinas controls with OIR (**Figure 5C**), consistent with proliferative endothelium and increased neovascularization. These results suggested that neuronal/glial Socs3 suppression increased pathologic VEGF-induced vascular endothelial cell proliferation.

To better understand how neuronal/glial *Socs3* controls VEGF production, we investigated which cell type could be a potential source of VEGF. The *nestin Cre* recombination appears in most neural and glial cells within the retina (15-17). We previously have demonstrated that in retinas with OIR, *Vegfa* mRNA is found in cell bodies identified morphologically as Müller cells (19). In addition, astrocyte-derived VEGF is essential for hypoxia-induced neovascularization (27). First we showed that cellular retinaldehyde binding protein (CralBP), a marker for Müller cells and astrocytes (28), co-localized with GFP which labels *nestin* Cre recombination in *Socs3 cKO; mTmG* reporter retinas with OIR (**Figure 6A**) indicating that *Socs3* was deleted in both Müller cells and astrocytes in *nestin* Cre driven *Socs3 cKO* retinas with OIR. Immunohistochemstry staining in *Socs3 cKO* retinas with OIR showed that VEGF and CralBP were colocalized in the RGC layer indicating that VEGF could be produced by CralBP-positive cells including Müller cells (end-feet) and astrocytes (**Figure 6B and 6C**). Glial fibrillary acidic protein (GFAP), a 51-kDa intermediate filament protein, is another marker for astrocytes, and activated Müller cell end-feet and processes (29). In this study we found that in *Socs3 cKO* retinas with OIR, Müller cells were highly activated, abundantly expressing GFAP (**Figure 6D**). Consistently, we found more GFAP-positive astrocytes in the RGC layer in *Socs3 cKO* retinas with OIR compared with littermate *Socs3 f/f* controls with OIR (**Figure 6E**). These data suggest that Müller cells and astrocytes might produce VEGF in addition to other neurons in RGC and INL layers.

Discussion

In this study we identified a neurovascular crosstalk pathway governing the progression of retinopathy. Specifically, neuronal/glial SOCS3 deficiency promotes pathologic retinal angiogenesis in retinopathy.

Socs3 expression was increased in the RGC layer and INL in wild type retinas with OIR. Neuronal/glial *Socs3* deficient mice with OIR had increased pathologic retinal neovascularization, but there was no affect on normal retinal vascular development (**Figure 2**) suggesting that neuronal/glial SOCS3 controls the pathological vascular response in retinopathy. Neuronal/glial SOCS3 loss suppressed inhibition of JAK, resulting in increased phosphorylation of STAT3 (**Figure 4C and D**) leading to increased *Vegfa e*xpression (**Figure 3**), increased endothelial cell proliferation and ERK activation (**Figure 5C**). These results suggest that neuronal/glial *Socs3* suppresses pathologic vascular endothelial cell proliferation by controlling VEGF secretion mediated by STAT3 activation.

In OIR, hyperoxia-induced retinal vessel loss is followed by hypoxia-induced increase in VEGF (30, 31), which contributes to pathologic neovascularization (18-20). Typically, the larger the area of vaso-obliteration, the greater the area of neovascularization, stimulated by hypoxia-regulated factors. Interestingly, in *Socs3 cKO* with OIR compared to *Socs3 f/f* mice with OIR at P17, the vaso-obliterated retinal area was reduced (though pathological neovascularization was increased). This is consistent with hypoxia-independent growth factor stimulation of endothelial cell proliferation (like VEGF controlled by phosophorylated STAT3 in our study), resulting in more revascularization and less vaso-obliteration, yet also resulting in more neovascularization, despite less hypoxia-driven neovascular growth. VEGF is a soluble factor that interacts with neurons, neuroglia and the vasculature affecting vascular development and neovascularization

(32). In OIR retinal neovascularization, *Vegf* mRNA has been localized to Müller cells in the INL layer of the retina (19), but the oxygen versus non-oxygen regulation of VEGF in Müller cells has not been well studied. Hypoxic conditions stabilize HIF-1α, allowing it to translocate from the cytosol to the nucleus (33), where it transcriptionally activates *Vegf* expression (22). Consistent with HIF-1α not being the only regulatory pathways for *Vegf* regulation in OIR, we found similar HIF-1α protein expression in both *Socs3 cKO* and *Socs3f/f* retinas with OIR and similar mRNA expression levels of other HIF-1α target genes that are involved in OIR and angiogenesis, such as *Epo* (34, 35), *Anptl4* (36, 37), *Ang1*, *PDGFα and TGFβ* (**Figure 4A and 4B**).

We found that increased phosphorylation of STAT3 was correlated with increased VEGF levels in the neuronal/glial *Socs3* deficient retinas with OIR (**Figure 4**), suggesting that neuroglial cell-secreted VEGF could be regulated by the SOCS3-JAK-STAT3 pathway. STAT3 and HIF-1α can cooperatively activate HIF-1α target genes including VEGF in tumor cells (38). In our study, increased VEGF in neuronal/glial *Socs3* deficient retinas appeared to be activated primarily by STAT3 and perhaps to a much lesser extent by HIF-1α.

In the OIR mouse model, in addition to VEGF, nerve growth factor (which is encoded by *Ngf*) contributes to retinal neovascularization through TrkA activation, which is attenuated by inhibition of Trk receptors (39). There was no significant difference in *Ngfβ* expression between *Socs3 cKO* and *Socs3 f/f* control retinas with OIR at P17 (**Figure S1**) suggesting that differences in neovascularization were not attributable to *Ngf* regulation.

Socs3 transcription is regulated by the Foxo family including Foxo3a and this regulation is feedback controlled by cytokines (40, 41). We found that mRNA expression of both Foxo1 and Foxo3a were similar in *Socs3 cKO* and *Socs3 f/f* control retinas with OIR at P17 suggesting that the Socs3/Foxo pathway was not affected by neuronal/glial *Socs3* deficiency (**Figure S2**).

SOCS3 is a major regulator of inflammation. The inflammatory factors, *IL-6*, *Il-1β* and *TNFα* involved in retinal neovascularization were all increased in *Socs3 cKO* retinas with OIR compared with *Socs3 f/f* controls (**Figure S3**). Since cytokines like *IL-6* also can induce VEGF production (42), increases in cytokines induced by neuronal/glial *Socs3* deficiency might also contribute to increased VEGF expression in *Socs3 cKO* retinas with OIR.

Identifying the molecular mechanisms underlying neurovascular cross talk is an important step in understanding pathologic proliferative retinopathy. Neuronal/glial SOCS3 suppresses neuronal/glial VEGF production to decrease vascular endothelial cell proliferation in the context of retinopathy, but not in retinal vascular development.

Materials and Methods

Animals

All animal studies were approved by the Institutional Animal Care and Use Committee at the Boston Children's Hospital. *Nestin Cre* expressing C57Bl/6 mice (Jackson Laboratory, stock # 003771) were crossed with *Socs3 flox/flox (Socs3 f/f)* mice (kind gift of Dr. A. Yoshimura) to generate *Socs3* conditional knockout mice *(Socs3 cKO)* and littermate control flox mice. $ROSA^{mTmG}$ reporter mice were from the Jackson Laboratory (stock# 007576). C57Bl/6 mice were from the Jackson Laboratory (stock # 000664).

Oxygen-induced retinopathy (OIR) and vessel quantification

OIR was induced in neonatal mice as described (14). Briefly, mouse pups with their nursing mothers were exposed to 75% oxygen from postnatal day (P) 7 to 12, then returned to room air until P17 (**Figure 1A**). The retinas were collected at P17 followed by staining overnight with

fluorescent *Griffonia Simplicifolia* Isolectin IB_4 (Invitrogen) and flat mounting. The avascular (vaso-obliteration) and pathologic neovascularization areas were quantified (43) using Adobe Photoshop (Adobe Systems) and Image J (National Institutes of Health, http://imagej.nih.gov/ij/). Mice with bodyweight less than 5 grams at P17 were excluded from the study (44).

In vivo imaging using Optical Coherence Tomography (OCT)

Mice were anesthetized with a mixture of xylazine (6 mg/kg) and ketamine (100 mg/kg), and pupils were dilated with a topical drop of Cyclomydril (Alcon Laboratories, Fort Worth, TX). Two minutes after pupil dilation, lubricating eye drops (Alcon Laboratories) were applied to the cornea. Spectral domain optical coherence tomography (SD-OCT) with guidance of the bright-field live fundus image was performed using the image-guided OCT system (Micron IV, Phoenix Research Laboratories) according to the manufacturer's instruction and using the vendor's image acquisition software to generate fundus images and OCT scans. The vendor's software Insight was used to measure the thickness of retinal layers (Nerve fiber layer (NFL)+IPL, INL) and entire retinas. The thickness of retinal layers was plotted at 4 distances from the optic nerve head (100, 200, 300, 400 μm).

Laser capture microdissection, RNA Isolation and quantitative RT-PCR

Cross-sectional retinal layers were laser microdissected according to manufacturer's instructions (Leica LMD6000). Briefly, eyes were enucleated from C57Bl/6J wild type mice at P17 in either OIR or normoxic conditions and embedded. 8 μm sections were isolated using a cryostat, mounted on ribonuclease (RNase)-free polyethylene naphthalate glass slides (Leica Microsystems; Wetzlar, Germany), followed by fixation in 50% ethanol for 15 seconds, and 30 seconds in 75% ethanol, before being washed with diethyl pyrocarbonate-treated water for 15

seconds. Sections were treated with RNase inhibitor (Roche) at 25 °C for 3 minutes. Retinal layers were then laser-capture microdissected with the Leica LMD 6000 system (Leica Microsystems) and collected directly into lysis buffer from the RNeasy Micro kit (Qiagen) followed by RNA isolation. Isolated RNA from whole retinas or laser-captured retinal layers using RNeasy kit (Qiagen) was reverse transcribed with M-MLV reverse transcriptase (Invitrogen) to generate cDNA. Quantitative RT-PCR was performed using a 7300 system (Applied Biosystems) with KAPA SYBR FAST qPCR Kits (Kapa Biosystems). *Cyclophilin A* was used as an internal control.

Immunohistochemistry

Immunostaining of retinas was performed as described (Chen et al., 2013). Briefly, eyes were isolated from P17 mice with OIR, fixed and permeabilized. The flat-mounted retinas or cross sections were stained with isolectin IB_4 (Invitrogene, 121413), anti-GFAP (Abcam, ab4674), anti-CralBP (Thermo, MA1-813), anti-phosphorylated STAT3 (Cell Signaling, M9C6, 4113), anti-VEGFA (R&D System, AF-493-NA) and DAPI (Invitrogene, D3571), and imaged using a confocal laser-scanning microscope (FV1000; Olympus).

Immunoblot

A standard immunoblotting (IB) protocol was used. Briefly, 300 mM NaCl, 0.5% NP-40, 50mM Tris.HCl pH7.4, 0.5 mM EDTA was used to lyse the retinas. Proteinase and phosphatase inhibitor cocktails were added. The antibodies used were: anti-phosphorylated ERK (Cell Signaling, 4376), anti-ERK (Cell Signaling, 4695), anti-phosphorylated STAT3 (Cell Signaling, 9131S), anti-STAT3 (Cell Signaling, 9132), β-ACTIN (Sigma, A1978).

Statistical analysis

Statistical analyses were performed with GraphPad Prism (v6.0) (GraphPad Software, Inc., San Diego, CA) and the results were compared using the Mann-Whitney test. P values <0.05 were considered statistically significant.

References

1. Guo S, Kim WJ, Lok J, Lee SR, Besancon E, Luo BH, Stins MF, Wang X, Dedhar S, and Lo EH. Neuroprotection via matrix-trophic coupling between cerebral endothelial cells and neurons. *Proceedings of the National Academy of Sciences of the United States of America.* 2008;105(21):7582-7.
2. Iadecola C. Neurovascular regulation in the normal brain and in Alzheimer's disease. *Nature reviews Neuroscience.* 2004;5(5):347-60.
3. Nishijima T, Piriz J, Duflot S, Fernandez AM, Gaitan G, Gomez-Pinedo U, Verdugo JM, Leroy F, Soya H, Nunez A, et al. Neuronal activity drives localized blood-brain-barrier transport of serum insulin-like growth factor-I into the CNS. *Neuron.* 2010;67(5):834-46.
4. Kern TS. Interrelationships between the Retinal Neuroglia and Vasculature in Diabetes. *Diabetes & metabolism journal.* 2014;38(3):163-70.
5. Nakahara T, Mori A, Kurauchi Y, Sakamoto K, and Ishii K. Neurovascular interactions in the retina: physiological and pathological roles. *Journal of pharmacological sciences.* 2013;123(2):79-84.
6. Qian H, and Ripps H. Neurovascular interaction and the pathophysiology of diabetic retinopathy. *Experimental diabetes research.* 2011;2011(693426.
7. Hellstrom A, Smith LE, and Dammann O. Retinopathy of prematurity. *Lancet.* 2013;382(9902):1445-57.
8. Starr R, Willson TA, Viney EM, Murray LJ, Rayner JR, Jenkins BJ, Gonda TJ, Alexander WS, Metcalf D, Nicola NA, et al. A family of cytokine-inducible inhibitors of signalling. *Nature.* 1997;387(6636):917-21.
9. Lebel E, Vallieres L, and Rivest S. Selective involvement of interleukin-6 in the transcriptional activation of the suppressor of cytokine signaling-3 in the brain during systemic immune challenges. *Endocrinology.* 2000;141(10):3749-63.
10. Jiang Y, Zhang Q, Soderland C, and Steinle JJ. TNFalpha and SOCS3 regulate IRS-1 to increase retinal endothelial cell apoptosis. *Cellular signalling.* 2012;24(5):1086-92.
11. Smith PD, Sun F, Park KK, Cai B, Wang C, Kuwako K, Martinez-Carrasco I, Connolly L, and He Z. SOCS3 deletion promotes optic nerve regeneration in vivo. *Neuron.* 2009;64(5):617-23.
12. Stahl A, Joyal JS, Chen J, Sapieha P, Juan AM, Hatton CJ, Pei DT, Hurst CG, Seaward MR, Krah NM, et al. SOCS3 is an endogenous inhibitor of pathologic angiogenesis. *Blood.* 2012;120(14):2925-9.
13. Marine JC, McKay C, Wang D, Topham DJ, Parganas E, Nakajima H, Pendeville H, Yasukawa H, Sasaki A, Yoshimura A, et al. SOCS3 is essential in the regulation of fetal liver erythropoiesis. *Cell.* 1999;98(5):617-27.
14. Smith LE, Wesolowski E, McLellan A, Kostyk SK, D'Amato R, Sullivan R, and D'Amore PA. Oxygen-induced retinopathy in the mouse. *Investigative ophthalmology & visual science.* 1994;35(1):101-11.

15. Arnold TD, Ferrero GM, Qiu H, Phan IT, Akhurst RJ, Huang EJ, and Reichardt LF. Defective retinal vascular endothelial cell development as a consequence of impaired integrin alphaVbeta8-mediated activation of transforming growth factor-beta. *The Journal of neuroscience : the official journal of the Society for Neuroscience.* 2012;32(4):1197-206.
16. Michan S, Juan AM, Hurst CG, Cui Z, Evans LP, Hatton CJ, Pei DT, Ju M, Sinclair DA, Smith LE, et al. Sirtuin1 over-expression does not impact retinal vascular and neuronal degeneration in a mouse model of oxygen-induced retinopathy. *PloS one.* 2014;9(1):e85031.
17. Chen J, Michan S, Juan AM, Hurst CG, Hatton CJ, Pei DT, Joyal JS, Evans LP, Cui Z, Stahl A, et al. Neuronal sirtuin1 mediates retinal vascular regeneration in oxygen-induced ischemic retinopathy. *Angiogenesis.* 2013;16(4):985-92.
18. Alon T, Hemo I, Itin A, Pe'er J, Stone J, and Keshet E. Vascular endothelial growth factor acts as a survival factor for newly formed retinal vessels and has implications for retinopathy of prematurity. *Nature medicine.* 1995;1(10):1024-8.
19. Pierce EA, Avery RL, Foley ED, Aiello LP, and Smith LE. Vascular endothelial growth factor/vascular permeability factor expression in a mouse model of retinal neovascularization. *Proceedings of the National Academy of Sciences of the United States of America.* 1995;92(3):905-9.
20. Stone J, Chan-Ling T, Pe'er J, Itin A, Gnessin H, and Keshet E. Roles of vascular endothelial growth factor and astrocyte degeneration in the genesis of retinopathy of prematurity. *Investigative ophthalmology & visual science.* 1996;37(2):290-9.
21. Ferrara N, Houck K, Jakeman L, and Leung DW. Molecular and biological properties of the vascular endothelial growth factor family of proteins. *Endocrine reviews.* 1992;13(1):18-32.
22. Forsythe JA, Jiang BH, Iyer NV, Agani F, Leung SW, Koos RD, and Semenza GL. Activation of vascular endothelial growth factor gene transcription by hypoxia-inducible factor 1. *Molecular and cellular biology.* 1996;16(9):4604-13.
23. Wei X, Wang G, Li W, Hu X, Huang Q, Xu K, Lou W, Wu J, Liang C, Lou Q, et al. Activation of the JAK-STAT3 pathway is associated with the growth of colorectal carcinoma cells. *Oncology reports.* 2014;31(1):335-41.
24. Wei D, Le X, Zheng L, Wang L, Frey JA, Gao AC, Peng Z, Huang S, Xiong HQ, Abbruzzese JL, et al. Stat3 activation regulates the expression of vascular endothelial growth factor and human pancreatic cancer angiogenesis and metastasis. *Oncogene.* 2003;22(3):319-29.
25. Niu G, Wright KL, Huang M, Song L, Haura E, Turkson J, Zhang S, Wang T, Sinibaldi D, Coppola D, et al. Constitutive Stat3 activity up-regulates VEGF expression and tumor angiogenesis. *Oncogene.* 2002;21(13):2000-8.
26. Kuriyama M, Taniguchi T, Shirai Y, Sasaki A, Yoshimura A, and Saito N. Activation and translocation of PKCdelta is necessary for VEGF-induced ERK activation through KDR in HEK293T cells. *Biochemical and biophysical research communications.* 2004;325(3):843-51.
27. Weidemann A, Krohne TU, Aguilar E, Kurihara T, Takeda N, Dorrell MI, Simon MC, Haase VH, Friedlander M, and Johnson RS. Astrocyte hypoxic response is essential for pathological but not developmental angiogenesis of the retina. *Glia.* 2010;58(10):1177-85.
28. Xu XL, Lee TC, Offor N, Cheng C, Liu A, Fang Y, Jhanwar SC, Abramson DH, and Cobrinik D. Tumor-associated retinal astrocytes promote retinoblastoma cell proliferation through production of IGFBP-5. *The American journal of pathology.* 2010;177(1):424-35.
29. Chang ML, Wu CH, Jiang-Shieh YF, Shieh JY, and Wen CY. Reactive changes of retinal astrocytes and Muller glial cells in kainate-induced neuroexcitotoxicity. *Journal of anatomy.* 2007;210(1):54-65.

30. Stahl A, Connor KM, Sapieha P, Chen J, Dennison RJ, Krah NM, Seaward MR, Willett KL, Aderman CM, Guerin KI, et al. The mouse retina as an angiogenesis model. *Investigative ophthalmology & visual science.* 2010;51(6):2813-26.
31. Ozaki H, Yu AY, Della N, Ozaki K, Luna JD, Yamada H, Hackett SF, Okamoto N, Zack DJ, Semenza GL, et al. Hypoxia inducible factor-1alpha is increased in ischemic retina: temporal and spatial correlation with VEGF expression. *Investigative ophthalmology & visual science.* 1999;40(1):182-9.
32. Ferrara N, Gerber HP, and LeCouter J. The biology of VEGF and its receptors. *Nature medicine.* 2003;9(6):669-76.
33. Kallio PJ, Okamoto K, O'Brien S, Carrero P, Makino Y, Tanaka H, and Poellinger L. Signal transduction in hypoxic cells: inducible nuclear translocation and recruitment of the CBP/p300 coactivator by the hypoxia-inducible factor-1alpha. *The EMBO journal.* 1998;17(22):6573-86.
34. Jiang BH, Rue E, Wang GL, Roe R, and Semenza GL. Dimerization, DNA binding, and transactivation properties of hypoxia-inducible factor 1. *The Journal of biological chemistry.* 1996;271(30):17771-8.
35. Chen J, Connor KM, Aderman CM, and Smith LE. Erythropoietin deficiency decreases vascular stability in mice. *The Journal of clinical investigation.* 2008;118(2):526-33.
36. Xin X, Rodrigues M, Umapathi M, Kashiwabuchi F, Ma T, Babapoor-Farrokhran S, Wang S, Hu J, Bhutto I, Welsbie DS, et al. Hypoxic retinal Muller cells promote vascular permeability by HIF-1-dependent up-regulation of angiopoietin-like 4. *Proceedings of the National Academy of Sciences of the United States of America.* 2013;110(36):E3425-34.
37. Perdiguero EG, Galaup A, Durand M, Teillon J, Philippe J, Valenzuela DM, Murphy AJ, Yancopoulos GD, Thurston G, and Germain S. Alteration of developmental and pathological retinal angiogenesis in angptl4-deficient mice. *The Journal of biological chemistry.* 2011;286(42):36841-51.
38. Pawlus MR, Wang L, and Hu CJ. STAT3 and HIF1alpha cooperatively activate HIF1 target genes in MDA-MB-231 and RCC4 cells. *Oncogene.* 2014;33(13):1670-9.
39. Liu X, Wang D, Liu Y, Luo Y, Ma W, Xiao W, and Yu Q. Neuronal-driven angiogenesis: role of NGF in retinal neovascularization in an oxygen-induced retinopathy model. *Investigative ophthalmology & visual science.* 2010;51(7):3749-57.
40. Honda M, Takehana K, Sakai A, Tagata Y, Shirasaki T, Nishitani S, Muramatsu T, Yamashita T, Nakamoto Y, Mizukoshi E, et al. Malnutrition impairs interferon signaling through mTOR and FoxO pathways in patients with chronic hepatitis C. *Gastroenterology.* 2011;141(1):128-40, 40 e1-2.
41. Barclay JL, Anderson ST, Waters MJ, and Curlewis JD. Regulation of suppressor of cytokine signaling 3 (SOC3) by growth hormone in pro-B cells. *Molecular endocrinology.* 2007;21(10):2503-15.
42. Cohen T, Nahari D, Cerem LW, Neufeld G, and Levi BZ. Interleukin 6 induces the expression of vascular endothelial growth factor. *The Journal of biological chemistry.* 1996;271(2):736-41.
43. Connor KM, Krah NM, Dennison RJ, Aderman CM, Chen J, Guerin KI, Sapieha P, Stahl A, Willett KL, and Smith LE. Quantification of oxygen-induced retinopathy in the mouse: a model of vessel loss, vessel regrowth and pathological angiogenesis. *Nat Protoc.* 2009;4(11):1565-73.
44. Stahl A, Chen J, Sapieha P, Seaward MR, Krah NM, Dennison RJ, Favazza T, Bucher F, Lofqvist C, Ong H, et al. Postnatal weight gain modifies severity and functional outcome of oxygen-induced proliferative retinopathy. *The American journal of pathology.* 2010;177(6):2715-23.

Acknowledgements: We thank Dr. A. Yoshimura for the Socs3 flox/flox mice and thank

Christian Hurst, Aimee Juan, Dorothy Pei and Ricky Cui for their excellent technical assistance. We thank The Harvard Catalyst Biostatistical Consulting Program and Dr. Catherine Stamoulis for reviewing the raw data and selecting appropriate statistical methods used in the manuscript. We also thank the anonymous reviewers of previous versions of the manuscript for their helpful suggestions. **Funding**: This work was supported by the National Institutes of Health/National Eye Institute (EY022275, EY017017, P01 HD18655), Lowy Family Foundation, European Commission FP7 project 305485 PREVENT-ROP for LEHS; JC was supported by National Institutes of Health/National Eye Institute (R01 EY024963), Boston Children's Hospital (BCH) Career Development Award, BrightFocus Foundation, BCH Ophthalmology Foundation, Mass Lions Eye Research Fund Inc. and Alcon Research Institute. AS was supported by Deutsche Forschungsgemeinschaft (DFG STA 1102/5-1), Deutsche Ophthalmologische Gesellschaft (DOG). JSJ was supported by Burroughs Wellcome Fund Career Awards for Medical Scientists (CAMS), Foundation Fighting Blindness, Canadian Child Health Clinician Scientist Program and Fonds de recherche du Québec - Santé. **Author contributions:** Y.S., J.M., A.S., J.S.J., J.C., W.P., L.E.H.S., contributed to designing the experiments and interpreting the results. Y.S., J.M., Z.L., T.F., L.E., K.T., N.S., P.M. performed the experiments. Y.S., J.C., L.E.H.S., wrote the manuscript. **Competing interests**: The authors declare that they have no competing interests.

Figure legends

Figure 1. *Socs3* mRNA expression was induced in neuronal layers in the OIR model. (**A**) Schematic diagram of OIR. Neonatal mice were exposed to 75% oxygen from postnatal day (P) 7-12 to induce vessel loss and returned to room air from P12-P17 to induce maximum pathologic neovascularization at P17. (**B**) *Socs3* mRNA expression in P17 retinal layers from laser-capture-micro-dissection from retinas with OIR compared to age-matched normoxia (Norm) control retinas (n=6 retinas per group). *Socs3* mRNA was increased in the RGC layer (P=0.002) and INL (P=0.002), but not in the ONL in retinas with OIR compared with normoxia control retinas. Images on the left show representative retinal cross sections from normoxia and retinas with OIR stained with isolectin IB4 (red) for endothelial cells and DAPI (blue) (cell nuclei), with dotted lines highlighting the areas for laser-capture-micro-dissection. (**C**) *Socs3* was decreased 80% by crossing *Socs3 flox/flox (Socs3 f/f)* mice with *nestin-Cre* driven mice (*Socs3 cKO*). Decreased *Socs3* levels were confirmed in whole retinas by western blot (p=0.0022, n=6 per group). (**D**) P17 retinal cross sections from *Socs3 cKO;mTmG* retinas with OIR show that *Nestin*-driven Cre recombinase was present in all the neuronal layers (labeled with GFP) (n= 3 mice with 3 retinas per group). Scale bar: 100 μm.

Figure 2. Neuronal/glial *Socs3* attenuated pathologic neovascularization in mouse model with OIR. Representative retinal flat-mounts (**A, left panel**) from P17 *Socs3 f/f* and *Socs3 cKO* retinas with OIR stained with isolection IB4 (red). The areas of neovascularization and vaso-obliteration were highlighted for quantification (white) using Image J and Photoshop. Insets are enlarged pathologic neovessels. Quantification of pathologic neovascularization (**A, right panel**) showed *Socs3* attenuated pathologic neovascularization (p=0.004, n=10-27 retinas per group)

and decreased central vaso-obliteration areas in P17 retinas with OIR (p=0.016, n=10-27 retinas per group). Between *Socs3 f/f* and *Socs3 cKO* retinas, the retinal vaso-obliteration areas are comparable at P12 (p=0.18, n=6-10 retinas per group); there is no significant difference in: (**B**) normal developmental retina vascular areas at P7 (p=0.94, n=6 retinas per group); (**C**) three vessel layers in adults; (**D**) thicknesses of entire retina, INL and nerve fiber layer (NFL)+IPL layer in live mice (n=6 retinas per group) (**E**). Black arrows in fundus images indicate the position of OCT. The outline of the layers was generated using Insight software. Scale bar for flat mounts in **A**-**C**: 1000 μm; for inset in **A**: 100 μm; for cross section in **D**: 50 μm; for layers in **D**: 25 μm; for OCT in **E**: 50 μm. NV, neovascularization; VO, vaso-obliteration.

Figure 3. Neuronal/glial *Socs3* deficiency enhanced *Vegfa* expression. (A) *Vegfa* mRNA expression in retinal layers from laser-capture-micro-dissection from P17 retinas with OIR compared to age-matched normoxia (Norm) control retinas. *Vegfa* mRNA expression was increased in the RGC and INL, but not in the ONL in retinas layers from P17 retinas with OIR compared with age-matched normoxic control retinas (n= 6 retinas per group). *Socs3* suppression in retinal neurons and glia increased *Vegfa* mRNA expression (p=0.002, n=6 retinas per group) **(B)**. mRNA expression of *Vegfa* isoform 120 and 164, but not 188 (n=6 retinas per group) (**C**), and VEGFA-164 protein level (~3.5 fold, p=0.002, n= 6 retinas per group) (**D**) were increased in P17 *Socs3 cKO* retinas with OIR compared with control retinas. (**E**) Immunohistochemistry staining with VEGFA (VEGFA-164) showed increased VEGF expression mainly in the INL and RGC layers. Representative images were from 3 mice per group. Scale bar: 50 μm.

Figure 4 Knocking out *Socs3* in neurons and glia increased STAT3. (**A, B**) In P17 retinas with OIR, the mRNA expression of HIF-1α target genes *Epo, Angptl4, Ang1, PDGFα and TGFβ*

and HIF-1α protein expression were at comparable levels in *Socs3 cKO* retinas and littermate *Socs3 f/f* retinas (n=6 retinas per group). (**C)** In P17 retinas with OIR, representative western blots show that phosphorylated STAT3 (pSTAT3) was highly increased in *Socs3 cKO* retinas compared to *Socs3 f/f* retinas. Band densities for western blots were quantified using image J in the bottom panel (p=0.028, n=4 per group). **(D)** In P17 retinas with OIR, phosphorylated STAT3 (pSTAT3) was increased mainly in the INL and RGC layers. Cross-sections were stained with pSTAT3 (green) and DAPI (blue). Representative images were from 3 mice per group. Scale bar: 50 μm.

Figure 5. Neuronal/glial *Socs3* deficiency increased endothelial proliferation and Erk phosphorylation. (A) In P17 retinas with OIR, Ki67 positive cells proliferative cells were increased in *Socs3 cKO* retinas compared to *Socs3 f/f* control retinas. Cross-sections from P17 retinas with OIR were stained with Ki67 (green (proliferative cells)), isolectin IB4 (magenta (EC)) and cell nuclei with DAPI (blue). Scale bar: 25 μm. The pixels of Ki67 positive staining were quantified with select color range function in Photoshop CS6 in (n=6 retinas per group) (**B**). (**C**) In P17 retinas with OIR, representative western blots show that phosphorylated ERK (pERK) was highly increased in *Socs3 cKO* retinas compared to *Socs3 f/f* OIR retinas. Band densities for western blots were quantified using image J in the right panel (p=0.028, n=4 per group).

Figure 6. Neuronal/glial deficiency of *Socs3* activated Müller glial cells and astrocytes. (**A**) In P17 *Socs3 cKO;mTmG* reporter retinas with OIR, CralBP labeled Müller cells and astrocytes colocalized with GFP. Cross-sections were stained for Müller cells and astrocytes with anti-CralBP (magenta) and cell nuclei with DAPI (blue). White arrow: astrocytes or end-feet of activated Müller cells. Open arrowheads: activated Müller cells. Scale bar: 10 μm. Images are

representative of 3 mice per group. (**B**) Cross-sections from P17 *Socs3 cKO* retinas with OIR were stained with CralBP (magenta), VEGF (green) and DAPI (blue). VEGF colocalized with CralBP positive cells. Scale bar: 10 μm. (**C**) A diagram showing VEGF in the RGC and INL layers including activated astrocytes and Müller cells. (**D**) In P17 retinas with OIR, GFAP-labeled activated Müller cells in *Socs3 cKO* retinas were increased compared to *Socs3 f/f* control retinas. Cross-sections from P17 *Socs3 cKO* and *Socs3 f/f* control retinas with OIR were stained for endothelial cells with isolectin IB4 (magenta), activated Müller cells and astrocytes with anti-GFAP (green) and cell nuclei with DAPI (blue). Scale bar: 25 μm. (**E**) GFAP-labeled astrocytes and end-feet of activated Müller cells in flat-mounted P17 *Socs3 cKO* and *Socs3 f/f* retinas with OIR. The pixels of GFAP positive staining in (**C**) and (**D**) were quantified with select color range function in Photoshop CS6. Representative images in A, B, D, and E were from 6 retinas per group. White arrow: astrocytes or end-feet of activated Müller cells. Open arrowheads: activated Müller cells. Scale bar: 50μm.

Figure 1

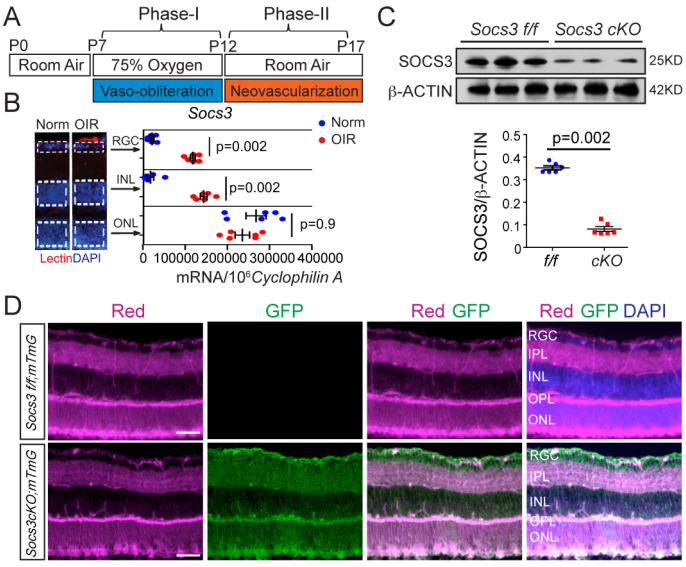
A
Phase-I
Phase-II
P0
P7
P12
P17
Room Air
75% Oxygen
Room Air
Vaso-obliteration
Neovascularization
B
Socs3
Norm
OIR
RGC
INL
ONL
p=0.002
p=0.002
p=0.9
Lectin
DAPI
0 100000 200000 300000 400000
mRNA/10^6 Cyclophilin A
C
Socs3 f/f
Socs3 cKO
SOCS3
β-ACTIN
25KD
42KD
SOCS3/β-ACTIN
p=0.002
0.5
0.4
0.3
0.2
0.1
0
f/f
cKO
D
Red
GFP
Red GFP
Red GFP DAPI
Socs3 f/f;mTmG
Socs3cKO;mTmG
RGC
IPL
INL
OPL
ONL

Figure 2

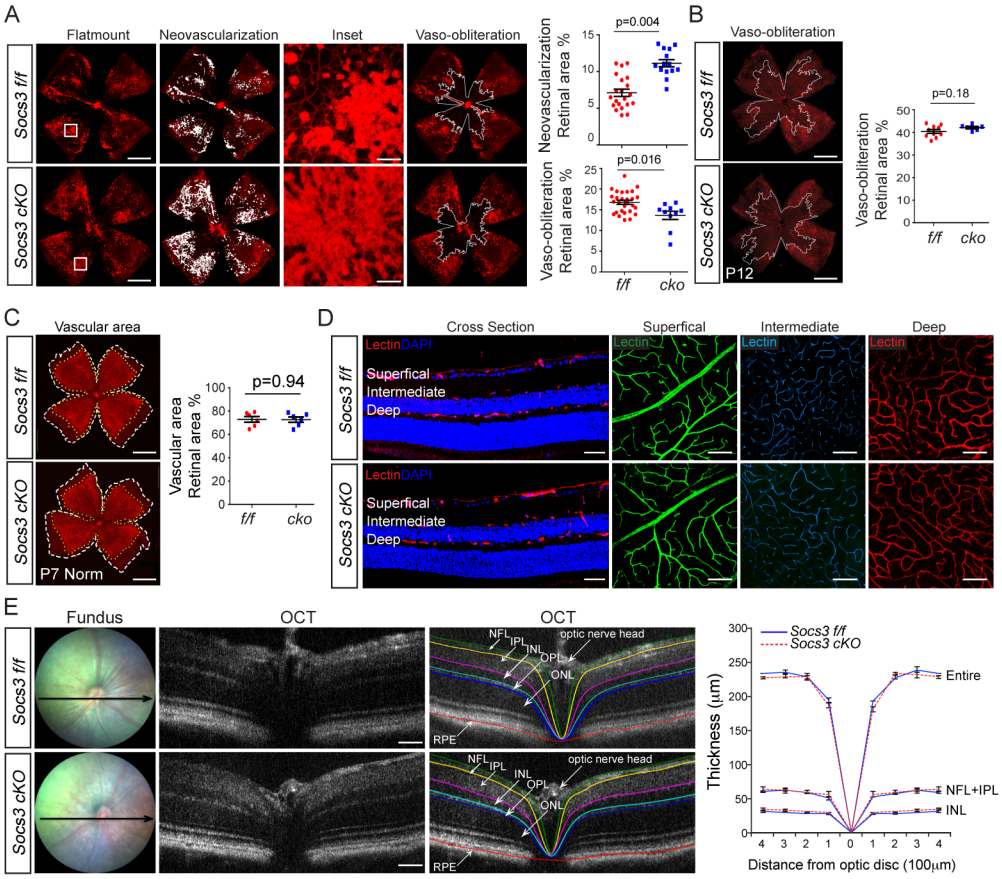
A
Flatmount
Neovascularization
Inset
Vaso-obliteration
Socs3 f/f
Socs3 cKO
Neovascularization Retinal area %
p=0.004
Vaso-obliteration Retinal area %
p=0.016
f/f
cko
B
Vaso-obliteration
P12
p=0.18
C
Vascular area
P7 Norm
Vascular area Retinal area %
p=0.94
D
Cross Section
Superfical
Intermediate
Deep
Lectin
DAPI
E
Fundus
OCT
NFL
IPL
INL
OPL
ONL
RPE
optic nerve head
Thickness (μm)
Entire
NFL+IPL
INL
Distance from optic disc (100μm)

Figure 3

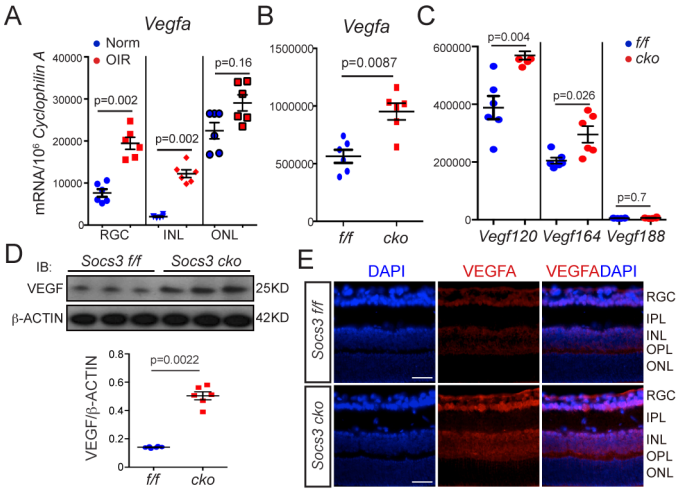
A
Vegfa
Norm
OIR
mRNA/10^6 Cyclophilin A
40000
30000
20000
10000
0
p=0.002
p=0.002
p=0.16
RGC
INL
ONL
B
Vegfa
1500000
1000000
500000
0
p=0.0087
f/f
cko
C
600000
400000
200000
0
p=0.004
p=0.026
p=0.7
f/f
cko
Vegf120
Vegf164
Vegf188
D
IB:
Socs3 f/f
Socs3 cko
VEGF
β-ACTIN
25KD
42KD
VEGF/β-ACTIN
0.8
0.6
0.4
0.2
0
p=0.0022
f/f
cko
E
DAPI
VEGFA
VEGFADAPI
Socs3 f/f
Socs3 cko
RGC
IPL
INL
OPL
ONL

Figure 4

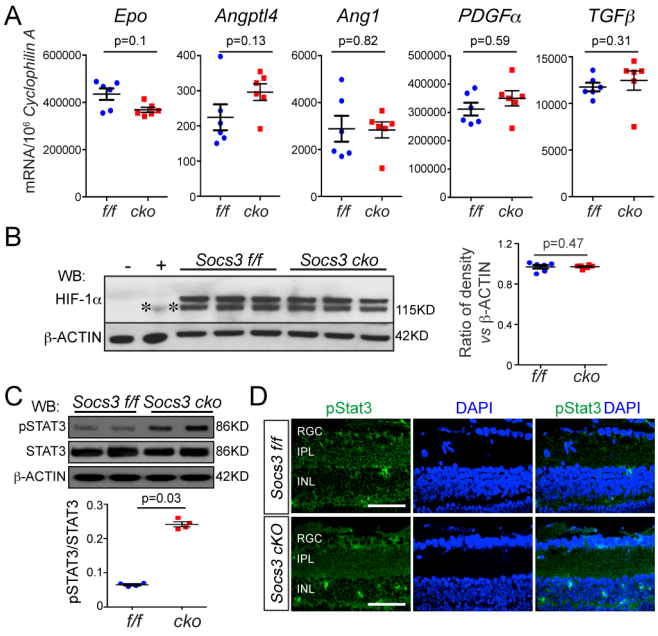
A
Epo
Angptl4
Ang1
PDGFα
TGFβ
p=0.1
p=0.13
p=0.82
p=0.59
p=0.31
mRNA/10^6 Cyclophilin A
f/f
cko
B
WB:
HIF-1α
β-ACTIN
Socs3 f/f
Socs3 cko
115KD
42KD
p=0.47
Ratio of density vs β-ACTIN
C
WB:
Socs3 f/f
Socs3 cko
pSTAT3
STAT3
β-ACTIN
86KD
86KD
42KD
p=0.03
pSTAT3/STAT3
D
pStat3
DAPI
pStat3 DAPI
Socs3 f/f
Socs3 cKO
RGC
IPL
INL

Figure 5

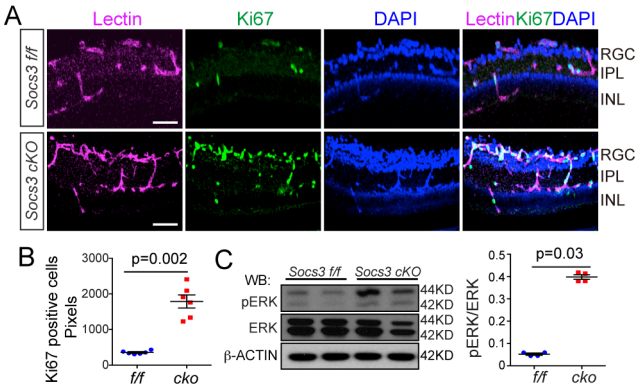
A
Lectin
Ki67
DAPI
LectinKi67DAPI
Socs3 f/f
Socs3 cKO
RGC
IPL
INL
RGC
IPL
INL
B
Ki67 positive cells
Pixels
3000
2000
1000
0
p=0.002
f/f
cko
C
WB:
Socs3 f/f
Socs3 cKO
pERK
ERK
β-ACTIN
44KD
42KD
44KD
42KD
42KD
pERK/ERK
0.5
0.4
0.3
0.2
0.1
0
p=0.03
f/f
cko

Figure 6

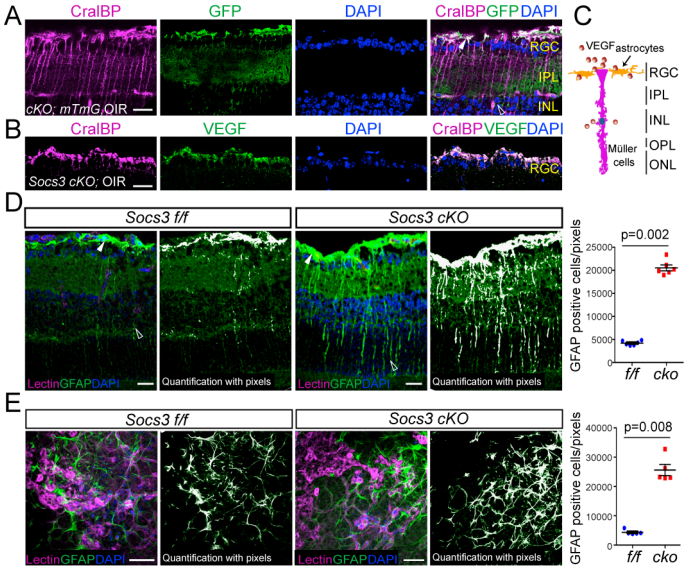
A
CralBP
GFP
DAPI
CralBPGFPDAPI
RGC
IPL
INL
cKO; mTmG OIR
B
CralBP
VEGF
DAPI
CralBPVEGFDAPI
RGC
Socs3 cKO; OIR
C
VEGF
astrocytes
RGC
IPL
INL
Müller cells
OPL
ONL
D
Socs3 f/f
Socs3 cKO
LectinGFAPDAPI
Quantification with pixels
GFAP positive cells/pixels
p=0.002
f/f
cko
E
Socs3 f/f
Socs3 cKO
LectinGFAPDAPI
Quantification with pixels
GFAP positive cells/pixels
p=0.008
f/f
cko